Astronomy & Astrophysics manuscript no. Corsi
May 11, 2009

© ESO 2009

arXiv:0905.1513v1 [astro-ph.CO] 11 May 2009

GeV emission from short Gamma-Ray Bursts: the case of GRB 081024B

Alessandra Corsi[1,2], Dafne Guetta[3], and Luigi Piro[2]

[1] Università degli studi di Roma “Sapienza” and INFN-Sezione di Roma, Piazzale Aldo Moro 2, 00185 Roma, Italy.
[2] INAF - Istituto di Astrofisica Spaziale e Fisica Cosmica di Roma, Via Fosso del Cavaliere 100, 00133 Roma, Italy.
[3] INAF - Osservatorio Astronomico di Roma, Via Frascati 33, 00040 Monte Porzio Catone, Italy

May 11, 2009

ABSTRACT

Aims. We investigate the origin of the high energy tail detected by Fermi/LAT in the short GRB 081024B through synchrotron and self-Compton emission in either the internal or external shock models.

Methods. In the internal shock scenario, we explore the possibility of generating the high energy photons directly through synchrotron process, or through inverse Compton emission in which target photons are synchrotron photons produced in internal shocks taking place either in the short prompt phase, or in a lately emitted shell (delayed internal shocks). In the external shock scenario, we consider the possibility of the high energy tail being the extension of the afterglow synchrotron emission, or alternatively the inverse Compton component associated to the afterglow synchrotron photons.

Results. For the internal shock scenario we conclude that, given the constraints set by the observations on the prompt emission spectrum, only an inverse Compton component from delayed internal shocks can accommodate the presence of a high energy tail extended up to the GeV range. In the external shock scenario, we show that interpreting the high energy tail as synchrotron-only afterglow emission, implies a bright late-time afterglow which was not observed by *Swift*. On the other hand, the observed high energy tail is consistent with an inverse Compton component of the afterglow, powered by a fireball with isotropic energy of the order of 10^{51} ergs, expanding in a uniform medium with density $n \sim 5$ particles/cm^3.

Key words. Gamma rays: bursts – X-rays: Individuals (GRB 081024B) – X-rays: bursts – radiation mechanisms: non-thermal

1. Introduction

Recent detection by the Fermi satellite of substantial high energy emission from short Gamma-Ray Bursts (GRBs, Omodei 2008; Ohno et al. 2009), calls for a reconsideration of this type of bursts as high energy sources. Such results are in fact surprising in the light of the expectations from before the launch of Fermi, when high energy emission was more likely expected in coincidence with long GRBs (see e.g. Abdo et al. 2009), because of the higher equivalent isotropic energy and interstellar medium (ISM) number density (Nakar 2007). However, Fermi observations of GRB 081024B point to the existence of a longer-lasting ($\sim$ 5 s) tail with few photons in the GeV range following the main event (Omodei 2008). Motivated by this recent result, we analyze here the conditions under which Fermi observations can be accommodated within the most popular theoretical models.

In the internal-external shock scenario of the fireball model (see e.g. Mészáros & Rees 1993; Sari et al. 1998), GRB prompt and afterglow emissions are thought to be produced by particles accelerated via shocks into an ultra-relativistic outflow (fireball) released during the burst explosion. While the prompt emission is related to shocks developing into the ejecta (internal shocks, IS), the afterglow arises from the forward external shock (ES) propagating into the ISM.

Synchrotron emission by the accelerated electrons is typically invoked as the main radiation mechanism. However, inverse Compton emission (IC) can also play an important role. Some synchrotron photons can in fact Compton scatter on the shock-accelerated electrons, producing an additional IC component at higher energies. This mechanism is also called synchrotron self-Compton (SSC) as the electrons responsible of the synchrotron emission are also responsible of the IC radiation. The ratio of IC-to-synchrotron luminosities is proportional to the square root of the ratio of the electron (ϵ_e) and magnetic (ϵ_B) energy densities behind the shock front. When this ratio is significantly above unity, the electron cooling rate via IC emission cannot be neglected.

IC emission from IS has been considered in various contexts (e.g. Papathanassiou & Mészáros 1996; Pilla & Loeb 1998; Ghisellini et al. 2000; Panaitescu & Mészáros 2000; Dai & Lu 2002; Guetta & Granot 2003; Baring & Braby 2004; Pe’er & Waxman 2004; Asano & Inoue 2007; Fan & Piran 2008; Galli & Guetta 2008; Li 2008; Yu & Dai 2009). Here we focus on the formulation given by Guetta & Granot (2003) where high-energy emission from internal shocks during the prompt GRB is computed, for both the synchrotron and IC components, as a function of two free parameters: the Lorentz factor Γ and the variability time t_v of the central engine that emits the outflow. IC emission from the ES (see e.g. Sari & Esin 2001; Zhang & Mészáros 2001, and references therein) has been invoked to explain GRB X-ray afterglows showing properties difficult to reconcile with the simplest synchrotron-only afterglow scenario (e.g. Wei & Lu 1998, 2000; Harrison et al. 2001; Corsi et al. 2005; Corsi & Piro 2006; Chandra et al. 2008), or in the context of higher energy emission from GRBs, in view of EGRET and Fermi/LAT capabilities and results (see

---

Send offprint requests to: alessandra.corsi@iasf-roma.inaf.it, guetta@oa-roma.inaf.it, luigi.piro@iasf-roma.inaf.it

e.g. Pe'er & Waxman 2005; Wang et al. 2006; Gou & Mészáros 2007; Galli & Piro 2007; You et al. 2007; Fan et al. 2008; Fan & Piran 2008; Galli & Piro 2008; Wang et al. 2009; Fan 2009).

The detection of GRB high energy (MeV to GeV) emission by AGILE and Fermi/LAT can be particularly relevant to probe the mechanisms active during the prompt-to-afterglow transition phase, when IC emission from both the IS and ES may be invoked, and observations are needed to discriminate between different models. In this context, we consider the case of the short GRB 081024B, for which a high energy emission tail was detected by the Fermi/LAT after the prompt phase. Zou et al. (2008) recently concluded that both the IS and ES scenarios could give rise to an emission peaking at GeV energies, in agreement with the observations for this burst. In this paper, we expand with more details the analysis by Zou et al. (2008). In the IS scenario, we consider the possibility that the $\sim$ GeV emission from GRB 081024B is due to (i) IC scatter of synchrotron photons emitted in the IS generating the GRB prompt emission, (ii) to the simple extension of the synchrotron spectrum in the GeV range, or (iii) to the up-scattering of soft X-ray photons emitted by late IS. The observations are used to derive constraints on the IS model parameters. For what concerns the ES scenario, we consider both the possibilities of explaining the high energy tail as simple extension to high energies of the afterglow synchrotron emission, or as the SSC component associated to the afterglow synchrotron photons. Constrains on the model are derived by taking into account not only the IC peak energy, which was considered by Zou et al. (2008), but also its luminosity, thus providing a quantitative estimate of its compatibility with the observations. Both the late IS and ES scenarios, can naturally account for a delay between the GRB trigger time and the longer-lasting high energy tail. Such property of these models is remarkable given the fact that a delay was indeed observed in some other cases (see e.g. Abdo et al. 2009).

2. Observations

At 21:22:40.86 UT on 24 October 2008, the Fermi Gamma-Ray Burst Monitor (GBM) triggered on GRB 081024B. This GRB had a duration of about 800 ms, and showed two main peaks (Connaughton et al. 2008). The first peak lasted $\sim$ 200 ms and its spectrum was in agreement with a cut-off power-law model, with a power-law index -0.70 ± 0.13, and an exponential cutoff at $E_{peak} = 1583 \pm 520$ keV. The second peak lasted $\sim$ 600 ms, and its spectrum was well fitted by a power-law model with index -1.28 ± 0.04 (Connaughton et al. 2008). The burst fluence in the 50-300 keV energy band was $(3.4 \pm 0.1) \times 10^{-7}$ ergs cm^{-2}, with a peak flux measured over a 64 ms timescale of 4.2 ± 0.2 photons cm^{-2} s^{-1}. In the 15-150 keV range, the 64 ms peak flux was measured to be 7.4 ± 0.4 photons cm^{-2} s^{-1} (Connaughton et al. 2008). The Fermi LAT telescope detected an increased count rate at 21:22:41 UT, associated with GRB 081024B. The emission from the point source was seen up to 3 GeV, in the first 5 s after the trigger (Omodei 2008).

GRB081024B triggered also the Suzaku Wide-band All-sky Monitor (WAM, 50 keV - 5 MeV) at $T_0 = 21:22:40.526$ UT (Hanabata et al. 2008). The light curve showed a double-peaked structure with a T_{90} duration of ~ 0.4 s. The fluence in 100 - 1000 keV range was $(2.7^{+0.7}_{-1.0}) \times 10^{-7}$ ergs cm^{-2}. The peak flux within 0.5 s was $1.1^{+0.3}_{-0.5}$ photons cm^{-2} s^{-1} in the same energy range. Preliminary results showed that at least 2 MeV photons were detected, and the time-averaged spectrum from T_0 to $T_0 + 0.5$ s was well fitted by a single power-law, with a photon index of $-1.24^{+0.25}_{-0.19}$ (Hanabata et al. 2008).

Swift XRT began observing the field of the Fermi-LAT around 70.3 ks after the trigger (Guidorzi et al. 2008a). Thanks to a series of follow-up observations (Guidorzi et al. 2008b,c), it was possible to establish that none of the three sources candidate as the GRB X-ray counterpart were fading.

3. Prompt high energy emission

In this section we consider the synchrotron and SSC emission in the framework of the IS model, following the prescriptions presented in Guetta & Granot (2003). In such model the flow Lorentz factor Γ is assumed to vary on a typical time scale t_v and with an amplitude $\delta\Gamma \sim \Gamma$. The shells collide at a radius $R \approx 2\Gamma^2 c t_v = 6 \times 10^{13} \Gamma^2_{2.5} t_{v,-2}$ cm, where $\Gamma_{2.5} = \Gamma/10^{2.5}$ and $t_{v,-2} = t_v/(10^{-2}$ s). The internal energy released in each collision is distributed among electrons, magnetic field and protons with fractions ϵ_e, ϵ_B and $(1-\epsilon_e)$ respectively. The electrons are accelerated in the shocks to a power-law distribution of energy $N(\gamma) \propto \gamma^{-p}$, and radiatively cool by the combination of synchrotron and SSC processes, the timescales of which are $t_{syn} \sim 6\pi m_e c/\sigma_T B^2 \gamma$ and $t_{SSC} = t_{syn}/Y$, the combined cooling time being $t_c = (1/t_{syn} + 1/t_{SSC})^{-1} = t_{syn}/(1+Y)$, where B is the magnetic field, and Y is the Compton y-parameter (Sari et al. 1996), $Y \approx \epsilon_e/\epsilon_B$ for $\epsilon_e << \epsilon_B$ and $Y \approx (\epsilon_e/\epsilon_B)^{1/2}$ for $\epsilon_e >> \epsilon_B$. The synchrotron peak energy is given by (Guetta & Granot 2003):

$$E_p = h\nu_m = \frac{0.12}{(1+z)}\left(\frac{3p-6}{p-1}\right)^2 (1+Y)^{-1/3} \epsilon_e^{3/2} \epsilon_B^{1/2} L_{52}^{1/2} \Gamma_{2.5}^{-2} t_{v,-2}^{-1} \text{ MeV} \tag{1}$$

Here L_{52} is the source peak luminosity in units of 10^{52} ergs (Guetta & Granot 2003), which is estimated as follows:

$$L = 4\pi d_L^2 \int_0^\infty F_\nu d\nu \simeq 4\pi d_L^2 \int_{50\text{keV}}^{1\text{MeV}} F_0 \left(\frac{\nu}{1\text{keV}}\right)^{-1.2} \nu d\nu \tag{2}$$

where we have considered that the burst spectrum had a cut-off energy $E_{peak} \sim 1$ MeV (Sec. 2); d_L is the luminosity distance to the source; F_0 is measured in units of photons cm^{-2} s^{-1} keV^{-1}. The last is estimated so as to have a peak flux in the $50-300$ keV energy range compatible with the observed one, i.e. (see also Sec. 2):

$$\int_{50\text{keV}}^{300\text{keV}} F_0 \left(\frac{\nu}{1\text{keV}}\right)^{-1.2} d\nu \simeq 4.2 \text{ photons cm}^{-2} \text{ s}^{-1} \tag{3}$$

Note that the spectral index of -1.2 is chosen as the temporal weighted mean of the spectral indices observed during the burst by GBM/Fermi and by Suzaku/WAM[1]. In such a way we get $L_{52} \sim 6.4 \times 10^{-3}$, for a burst located at $z = 0.1$. No afterglow emission was detected for GRB 081024B, so the burst redshift is unknown. Hereafter we assume $z = 0.1$ as a reference value for short GRBs.

According to what seen in Sec. 2, the observations constrain the peak of the synchrotron component to be at $\sim$ 1 MeV. From Eq. (1) it follows that for a given value of Γ, E_p is maximized by maximizing ϵ_e, ϵ_B and p, and by minimizing z and $t_{v,-2}$. As shown in Fig. 1, for $\Gamma_{2.5} = 1$, even setting $\epsilon_e \sim 0.5$, $\epsilon_B \sim 0.1$, $p = 2.5$, $z = 0.1$ and $t_{v,-2} = 0.01$[2], we get $E_p \sim 66$ keV $<< 1$ MeV

---

[1] $-1.2 \simeq (-0.7 \times 0.2 \text{ s} - 1.28 \times 0.6 \text{ s} - 1.24 \times 0.5 \text{ s})/(0.5 \text{ s} + 0.6 \text{ s} + 0.2 \text{ s})$

[2] Such short variability timescales can be present (Nakar 2007), and was indeed found in at least one short GRB, in which a very bright < 1 ms pulse was observed (Scargle et al. 1998).

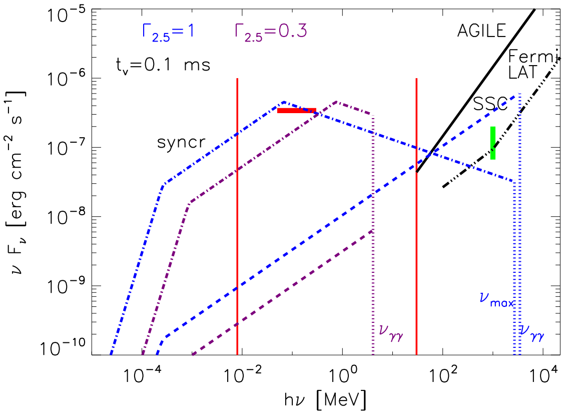

Fig. 1. Synchrotron (dot-dashed lines) and SSC (dashed lines) prompt emission spectra for a burst at $z = 0.1$. The prompt emission luminosity is $L_{52} = 6.4 \times 10^{-3}$ and we set $t_v = 0.1$ ms, $\epsilon_e = 0.5$, $\epsilon_B = 0.1$, and $p = 2.5$. We display the predicted spectra for $\Gamma_{2.5} = 1$ (blue) and $\Gamma_{2.5} = 0.3$ (purple). The solid and dot-dot-dot-dashed lines represent AGILE and Fermi/LAT sensitivity for an integration time of 10 s (see Galli & Piro 2007). The red solid vertical lines delimit the energy range (8 keV - 30 MeV) covered by the Fermi/GBM (NaI and BGO) detectors (http://fermi.gsfc.nasa.gov/science/instruments/gbm.html). The red solid horizontal line marks the level of the 50-300 keV fluence measured by the GBM during the ∼ 1 s duration of the prompt burst. The green solid vertical line marks the flux level at 1 GeV, assuming that a number of GeV photons in between 2 and 6 are detected in 5 s. See the electronic version of this paper for colors.

(dot-dashed blue line). Note that in this last figure we have indicated with $\nu_{max} = 9.5\,(1+z)^{-1}(1+Y)^{-1}\Gamma_{2.5}$ GeV, the maximum frequency of the synchrotron spectrum (Guetta & Granot 2003). Maintaining unchanged the values of the other parameters, we need $\Gamma_{2.5} = 0.3$ to have $E_p \sim 1$ MeV. The next step requires checking if, for this last set of parameters, the source is optically thin for pair production at energies as high as ∼ 1 GeV[3]. The cutoff energy for pair production reads (Guetta & Granot 2003):

$$E_{pair} = 2.6\,(1+z)^{-1}(\epsilon_e^3\epsilon_B)^{(2-p)/2p}L_{52}^{-(p+2)/2p}\Gamma_{2.5}^{4(p+1)/p}t_{v,-2}\text{ GeV} \quad (4)$$

From the above formula it turns out that lowering the value of Γ so as to have $E_p \sim 1$ MeV, lowers E_{pair} in such a way that there will be no substantial emission in the GeV range. We can show this clearly by expressing E_{pair} as a function of the peak energy of the synchrotron spectrum E_p. This is done by using Eq. (1) to derive Γ as a function of E_p, and then substituting into the above equation. In this way we get:

$$E_{pair} = \frac{2.6}{(1+z)^{(3p+2)/p}} \times \left[\frac{0.12\times\left(\frac{3p-6}{p-1}\right)^2}{(E_p/\text{MeV})(1+Y)^{1/3}}\right]^{2(p+1)/p} \times$$
$$\times\epsilon_e^{(3p+12)/2p}\,\epsilon_B^{(p+4)/(2p)}L_{52}^{1/2}t_{v,-2}^{-(p+2)/p}\text{ GeV} \quad (5)$$

We note that, for a given E_p and L_{52}, E_{pair} is maximized by maximizing ϵ_e, ϵ_B, and by minimizing z and $t_{v,-2}$. Setting $L_{52} = 6.4 \times 10^{-3}$, $t_{v,-2} = 10^{-2}$, $\epsilon_e = 0.5$, $\epsilon_B = 0.1$, $p = 2.5$, $z = 0.1$ and $E_p = 1$ MeV, we have $E_{pair} \sim 4$ MeV (see the purple dotted line in Fig. 1). In passing we note that the GeV emission of GRB 081024B would have been roughly compatible either with the extrapolation of the synchrotron spectrum, or with the additional contribution of an IC component (see Fig. 1). In the latter case, the SSC peak energy is (Guetta & Granot 2003):

$$E_p^{SC} = h\nu_m^{SC} = \frac{4.6\times10^4}{(1+z)}\left(\frac{3p-6}{p-1}\right)^4\epsilon_e^{7/2}\epsilon_B^{1/2}L_{52}^{1/2}\Gamma_{2.5}^{-2}t_{v,-2}^{-1}\text{ MeV} \quad (6)$$

However, as demonstrated above, the source is optically thick for GeV photons, thus we conclude that the observations of this burst are difficult to reconcile with either a simple extrapolation of synchrotron photons or first order IC scatter in the IS phase of the prompt emission[4].

4. Late high energy emission

4.1. Delayed emission from IS

Another mechanism which may be responsible for the ∼ GeV emission, is represented by the SSC component of an extended soft X-ray tail, produced by synchrotron emission from IS developing in some lately ejected shells (see also Zou et al. 2008). In this case, we estimate the typical X-ray luminosity of a short GRB by considering the 0.3 – 10 keV fluxes at 100 s, $F_{0.3-10keV,\ 100\ s}$, reported in Table 2 of Nakar (2007), that range in between 6×10^{-13} ergs cm^{-2} s^{-1} and 1.2×10^{-8} ergs cm^{-2} s^{-1}, with a mean value of $< F_{0.3-10\text{ keV},\ 100\text{ s}} >\simeq 2 \times 10^{-9}$ ergs cm^{-2} s^{-1}. The overall early X-ray emission of short GRBs has been observed to be somewhat different from the complex early X-ray afterglows of long GRBs. Short GRBs with extended X-ray tails have the end of such emission characterized by a steep decay, with a power-law index $\alpha \lesssim -2$, before a typical late afterglow decay ($\alpha \sim -1$) is observed (Nakar 2007). In other short bursts the regular X-ray decay ($\alpha \sim -1$) is observed starting at early times (Nakar 2007). We thus extrapolate $F_{0.3-10\text{keV},\ 100\text{ s}}$ to $t \sim 2.5$ s using a temporal index of $\alpha = -1.5$, somewhat in between the steep decay and the typical afterglow one. Note that since from the observations we know that the high energy tail of GRB 081024B lasted until ∼ 5 s after the GRB trigger, we are assuming here a reference time of 2.5 s (in the middle of the observed time interval). For $z = 0.1$, we get luminosities in between $\sim 4 \times 10^{45}$ ergs s^{-1} and $\sim 7\times10^{49}$ ergs s^{-1}, with a mean value of $\sim 10^{49}$ ergs s^{-1}. Setting $L_{52} = 10^{-3}$, $t_{v,-2} = 0.15$, $\epsilon_e = 0.45$, $\epsilon_B = 0.1$, $p = 2.5$, $z = 0.1$, $\Gamma_{2.5} = 0.43$, into Eqs. (1), (4), (6), we get $E_p \sim 10$ keV, $E_p^{SC} \sim 1$ GeV, and $E_{pair} > 1$ GeV, as shown in Fig. 2. As can be seen, in the late IS model the flux level of the high energy tail can be well

---

[3] Note that the suppression of emission due to the Klein-Nishima effect is relevant above $E_{KN} = h\nu_{KN}^{SC} = 100\frac{\Gamma_{2.5}^2}{E_p/\text{MeV}}$ GeV (Guetta & Granot 2003), which is much higher than E_{pair}.

[4] One may alternatively think that the high energy component observed in the LAT is generated by photons of the second prompt pulse, originating in a region spatially distinct from the first GBM pulse. The last, which lasted ∼ 200 ms, had a spectrum in agreement with a cut-off power-law with $E_{peak} = 1583 \pm 520$ keV, while the second pulse in the GRB light curve, that lasted 600 ms, had a spectrum consistent with a single power-law. The association of the LAT emission with the second pulse, together with the fact that during such pulse E_{peak} was no longer constrained by the GBM spectrum, would suggest $E_{peak} > 1$ MeV during the second pulse, so that the suppression due to pair production would become even worse (see Eq. (5)).

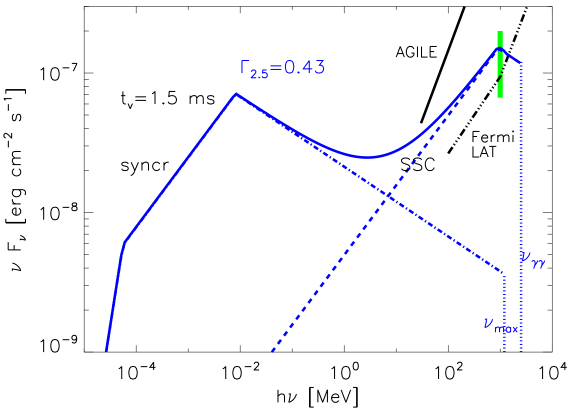

Fig. 2. Synchrotron (blue dot-dashed line) and SSC (blue dashed line) emission spectra from delayed IS for a burst with parameters $L_{52} = 10^{-3}$, $t_v = 1.5$ ms, $\epsilon_e = 0.45$, $\epsilon_B = 0.1$, $p = 2.5$, $z = 0.1$, $\Gamma_{2.5} = 0.43$. The blue solid line is the sum of the synchrotron and SSC contributions. The black solid and dot-dot-dot-dashed lines are the AGILE and Fermi/LAT sensitivity for an integration time of 10 s, respectively (see Galli & Piro 2007). For this choice of parameters one has a synchrotron peak around 10 keV and an SSC peak around ∼ 1 GeV. The green solid vertical line marks the flux level at 1 GeV, assuming that a number of GeV photons in between 2 and 6 are collected by the Fermi/LAT in 5 s. See the electronic version of this paper for colors.

above the LAT detection threshold. Thus, such model is a viable explanation for the LAT observations of this burst.

4.2. High energy emission from the ES

The high energy tail observed in GRB 081024B could also be produced in an extended X-ray tail associated, in this case, to synchrotron afterglow emission by the ES, or alternatively to an afterglow SSC component. In what follows, we explore both these possibilities.

4.2.1. Synchrotron-only scenario

Consider the case in which the high energy tail observed by the Fermi/LAT is the extension to high energies of the synchrotron component generating the afterglow. In this scenario, the afterglow synchrotron emission should match the 1 GeV flux level necessary to have few photons detected by the LAT, while in the $50-300$ keV energy range its flux should be below the value of $\sim 3.4\times10^{-7}$ ergs cm^{-2} observed in the ∼ 1 s duration of the burst by the GBM (see Sec. 2). To this end, the νF_ν spectrum should be sufficiently flat. I.e., assuming to have no spectral breaks between 50 keV and 1 GeV, and a spectral index of $1-p/2$ (as typically expected for the high energy part of the synchrotron spectrum, see e.g. Sari et al. 1998), a 1 GeV flux of 10^{-7} ergs cm^{-2} s^{-1}, and a flux at 175 keV (in the middle of the GBM band) constrained to be below $\sim 3.4\times10^{-7}$ ergs cm^{-2} s^{-1}, would imply $p < 2.3$. Such constrain on p results in a temporal decay of the X-ray light curve flatter than $-3/4(p-1)-1/4\sim-1.22$ (Sari et al. 1998). In an exposure spanning from 70.3 ks to 1.3×10^6 s after the burst, *Swift*/XRT observed the Fermi-LAT error circle, detecting three sources with average count rates below $\sim 2\times10^{-3}$ counts/s (Guidorzi et al. 2008d), that we estimate to correspond to an average $0.3-10$ keV flux of $\sim 8\times10^{-14}$ ergs cm^{-2} s^{-1}. These sources were excluded as X-ray counterparts of GRB 081024B, because they did not fade. We can thus use their flux level as an upper-limit for the afterglow flux of GRB 081024B at late times. In a synchrotron-only scenario with $p = 2.3$, the expected 5 keV flux (in the middle of the $0.3-10$ keV XRT band) at 1 day after the burst would be of the order of $(5\text{ keV}/10^6\text{ keV})^{1-2.3/2}\times(86400\text{ s}/2.5\text{ s})^{-1.22}\times10^{-7}$ ergs cm^{-2} s^{-1} $\sim 2\times10^{-12}$ ergs cm^{-2} s^{-1} $> 8\times10^{-14}$ ergs cm^{-2} s^{-1}. We thus conclude that, to explain the Fermi/LAT observations as synchrotron emission from the FS, one should have observed a bright late-time afterglow, contrary to *Swift*/XRT observations.

4.2.2. Synchrotron plus SSC scenario

Synchrotron component Following the prescriptions given by Sari & Esin (2001), we can write down the characteristic break frequencies and the peak flux of the synchrotron component as follows:

$$\nu_m = 5\times10^{12}\text{ Hz }(1+z)^{1/2}\frac{f(p)}{f(2.2)}\left(\frac{\epsilon_B}{0.01}\right)^{1/2}\left(\frac{\epsilon_e}{0.5}\right)^{2}E_{52}^{1/2}t_{day}^{-3/2} \quad (7)$$

where $f(p) = ((p-2)/(p-1))^2$,

$$\nu_c = \frac{2.7\times10^{15}}{(1+z)^{1/2}}\text{ Hz }\left(\frac{\epsilon_B}{0.01}\right)^{-3/2}E_{52}^{-1/2}n_1^{-1}t_{day}^{-1/2}(1+Y)^{-2} \quad (8)$$

$$f_m = 2.6\text{ mJy }(1+z)\left(\frac{\epsilon_B}{0.01}\right)^{1/2}E_{52}\,n_1^{1/2}d_{L,28}^{-2} \quad (9)$$

Here the fireball parameters are defined as usual: p is the index of the power-law electron energy distribution; ϵ_e is the ratio of the energy in electrons to the post-shock energy in nucleons; ϵ_B is the ratio of the magnetic field energy density to the post-shock nucleon energy density; E_{52} is the initial blast wave energy (in units of 10^{52} ergs); n_1 is the ambient number density (in units of particles/cm^3). As in the previous sections, $Y = \frac{L_{IC}}{L_{syn}}$, and *in the fast cooling regime* $Y\sim\sqrt{\frac{\epsilon_e}{\epsilon_B}}$ (e.g. Sari & Esin 2001). *In such a regime* the energy spectrum νF_ν peaks at ν_m, and thus $Y\sim(\nu_m^{IC}f^{IC}(\nu_m^{IC}))/(\nu_m f(\nu_m))$, where

$$L^{syn} = \nu_m(\nu_m/\nu_c)^{-1/2}f_m = 4.3\times10^{-13}\,\frac{\text{ergs}}{\text{cm}^2\text{ s}^1}\times$$
$$\times\left(\frac{f(p)}{f(2.2)}\right)^{1/2}(1+z)\left(\frac{\epsilon_e}{0.5}\right)^{1/2}\left(\frac{\epsilon_B}{0.01}\right)^{1/2}E_{52}t_{day}^{-1}d_{L,28}^{-2} \quad (10)$$

having used Eqs. (7)-(8), and $(1+Y)^{-2}\sim Y^{-2}=\epsilon_B/\epsilon_e$. If the peak of the synchrotron component in the νF_ν space is below 1 keV, i.e. if $\nu_m < 1$ keV, we can substitute L^{syn} on the left hand side of the above equation with the following expression:

$$L^{syn} = F^{syn}_{1keV}\left(\frac{\text{ergs}}{\text{cm}^2\text{ s Hz}}\right)(2.41\times10^{17}\text{ Hz})^{p/2}(\nu_m(\text{Hz}))^{-p/2+1} \quad (11)$$

In this way, from Eqs. (7) and (10)-(11) we derive the following expressions for ϵ_e and ϵ_B:

$$\epsilon_B = \frac{0.2}{(1+z)^{7/3}} \left(\frac{f(p)}{f(2.2)}\right)^{-2/3} \left(\frac{\nu_m}{1\mathrm{keV}}\right)^{-4p/3+2} \times \times \left(\frac{F^{syn}_{1\mathrm{keV}}}{10\ \mathrm{mJy}}\right)^{8/3} \left(\frac{t_s^5 d^{16}_{L,28}}{E^7_{52}}\right)^{1/3} \quad (12)$$

$$\epsilon_e = 0.01 \left(\frac{f(p)}{f(2.2)}\right)^{-1/3} \left(\frac{\nu_m}{1\mathrm{keV}}\right)^{p/3} \left(\frac{F^{syn}_{1\mathrm{keV}}}{10\ \mathrm{mJy}}\right)^{-2/3} \times \times \left(\frac{(1+z)E_{52}t_s}{d^4_{L,28}}\right)^{1/3} \quad (13)$$

The above equations allow us to eliminate from the problem the two unknown micro-physical parameters by expressing them as a function of the synchrotron peak frequency ν_m and the observed 1 keV flux. As seen in Sec. 4.1, we can set $< F_{0.3-10\ \mathrm{keV},\ 100\ \mathrm{s}} >\simeq 2\times10^{-9}$ ergs cm^{-2} s^{-1}. For $p = 2.05$ (so as to favor the emission at high energies by having a flat spectrum), we can estimate $F_{1\ \mathrm{keV},\ 2.5\ \mathrm{s}}$ by using a spectral slope of $\beta = -p/2 \sim -1$ in the 0.3 – 10 keV range (i.e. assuming to have $\nu_m \lesssim 0.3$ keV), and a temporal decay index of $\alpha = -3/4(p-1) - 1/4 \sim -1$. Doing so, it turns out that $F_{1\ keV,\ 2.5\ s} \sim 10$ mJy is a reasonable estimate. To constrain E_{52}, we use the 50−300 keV observed fluence, and assume that something like 3 photons are collected at ∼ 1 GeV by the Fermi/LAT in the 5 s energy tail. Setting $z = 0.1$, the isotropic energy into the fireball should be $E_{52} \gtrsim E_{\gamma,52} = 2\times10^{-3}$.

IC component In the fast cooling regime, the IC energy emission peaks at

$$\nu^{IC}_m = 2\gamma^2_m\nu_m = 3.7\ \mathrm{GeV} \left(\frac{f(p)}{f(2.2)}\right)^{1/3} \left(\frac{\nu_m}{1\mathrm{keV}}\right)^{2p/3+1} \times \times \left(\frac{F^{syn}_{1\mathrm{keV}}}{10\ \mathrm{mJy}}\right)^{-4/3} E^{11/12}_{52} n_1^{-1/4} t_s^{-1/12} (1+z)^{17/12} d^{-8/3}_{L,28} \quad (14)$$

where we have used (Sari & Esin 2001):

$$\gamma_m = 930 \left(\frac{f(p)}{f(2.2)}\right)^{1/2} \left(\frac{\epsilon_e}{0.5}\right) \left(\frac{E_{52}}{n_1}\right)^{1/8} \left(\frac{t_{day}}{1+z}\right)^{-3/8} \quad (15)$$

together with Eqs. (12)-(13). Setting $p = 2.05$, $E_{52} = 0.35$, $z = 0.1$, $n_1 = 5$, $\nu_m = 0.15$ keV, $F^{syn}_{1\mathrm{keV}} = 10$ mJy, $t = 2.5$ s in the above equation, we get $\nu^{IC}_m \sim 1$ GeV (see Fig. 3). Note that $E_{52} = 0.35$, compared to $E_{\gamma,52} = 2\times10^{-3}$ that can be estimated from the prompt and high energy tail fluence, requires a value for the conversion efficiency into γ-rays of the order of ∼ 1%, which is at the lower end of the typical range 0.01 – 1 found for long GRBs and suggested to be the same also for short GRBs (see e.g. Nakar 2007; Zhang et al. 2007). The IC flux at the peak ν^{IC}_m is given by:

$$\nu^{IC}_m f^{IC}(\nu^{IC}_m) = YL^{syn} = 5.3\times10^{-9}\frac{\mathrm{ergs}}{\mathrm{cm^2 s}} \left(\frac{f(p)}{f(2.2)}\right)^{1/6} \times \times \left(\frac{\nu_m}{1\ \mathrm{keV}}\right)^{p/3} \left(\frac{F^{syn}_{1\mathrm{keV}}}{10\ \mathrm{mJy}}\right)^{-2/3} (1+z)^{4/3} E^{4/3}_{52} t_s^{-2/3} d^{-10/3}_{L,28} \quad (16)$$

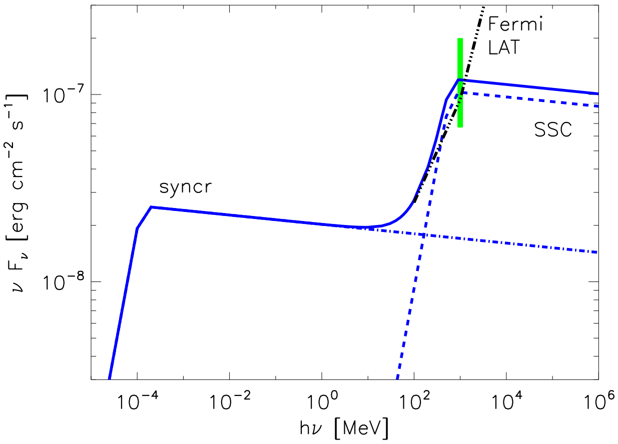

Fig. 3. Synchrotron (dot-dashed line) and SSC (dashed line) spectra in the ES scenario, for a burst with parameters $p = 2.05$, $E_{52} = 0.35$, $z = 0.1$, $n_1 = 5$, $\nu_m = 0.15$ keV, $F^{syn}_{1\mathrm{keV}} = 10$ mJy, $t_s = 2.5$. The solid line is the sum of the synchrotron and SSC contributions. For such choice of parameters one has an SSC peak around ∼ 1 GeV. The dot-dot-dot-dashed line represents the Fermi/LAT sensitivity for an integration time of 10 s (see Galli & Piro 2007). The green solid vertical line marks the flux level at 1 GeV, assuming that a number of photons in between 2 and 6 are collected in 5 s by the Fermi/LAT. See the electronic version of this paper for colors.

where we have used Eqs. (10), (12)-(13). For the same set of parameters we have $\nu^{IC}_m f^{IC}(\nu^{IC}_m) \sim 10^{-7}$ ergs cm^{-2} s^{-1} (see Fig. 3), which is comparable with the LAT sensitivity for 10 s integration time. Note that for a given value of ν_m, $F^{syn}_{1\mathrm{keV}}$, and z, the above equation constraints E_{52} to be sufficiently high for having the high energy tail visible by the Fermi/LAT. At the same time, looking at Eq. (14), it is evident that a higher value of E_{52} tends to shift the peak energy to higher values, so that to keep it around ∼ 1 GeV, n cannot be too low. Our value of $n = 5$ cm^{-3} is in the range that has been found to possibly characterize other short bursts (see e.g. Panaitescu 2006), and roughly at the higher edge of the 0.01 – 1 cm^{-3} range expected for an ISM.

Consistency checks: micro-physics, deceleration/cooling time and Klein-Nishina limit In order for the ES scenario proposed in this section being a self-consistent explanation of the high energy tail observed in GRB 081024B, we need to perform a series of checks to verify that the hypotheses under which we are working are consistently verified for our choice of parameters. First of all, the implied values of ϵ_e and ϵ_B should both be less than unity, and we should have $\epsilon_e >> \epsilon_B$. With our choice of parameters we get $\epsilon_B = 5.2\times10^{-3}$ and $\epsilon_e = 8.8\times10^{-2}$, that verify these conditions.

Next, in order to have an ES, we need the deceleration phase to be starting before or around the time at which the high energy tail is observed, i.e. (Sari & Piran 1999):

$$t_{dec} \sim 3.2\ \mathrm{s} \left(\frac{E_{52}}{n_1}\right)^{1/3} \left(\frac{\Gamma_0}{350}\right)^{-8/3} (1+z) \lesssim 2.5\mathrm{s} \quad (17)$$

which for $z = 0.1$, $E_{52} = 0.35$, and $n_1 = 5$, implies having $\Gamma_0 \gtrsim 285$, that is a reasonable lower-limit for the initial fireball Lorentz factor.

Moreover, we have been working under the hypothesis of being in the fast cooling regime, so we need to verify that this is indeed the case, i.e. $\nu_c(2.5\mathrm{s}) < \nu_m(2.5\mathrm{s})$. Using Eq. (8) we get $\nu_c(2.5\mathrm{s}) \sim 0.1$ keV, so the fast cooling hypothesis is also verified, and the fast-to-slow cooling transition takes place at about 3.6 s after the burst.

Finally, we need to check that the Klein-Nishina effect does not suppress the IC component. In the fast cooling regime, most of the synchrotron energy is emitted around ν_m and most of the SSC energy is emitted by electrons with $\gamma_e \sim \gamma_m$ that up-scatter photons with $\nu \sim \nu_m$. Therefore, the Klein-Nishina limit can be neglected only if (see e.g. Nakar 2007):

$$\nu_m \lesssim \nu_{KN}(\gamma_m) = \frac{m_e c^2 \Gamma}{\gamma_m} \tag{18}$$

Since $\gamma_m = (m_p/m_e)(f(p))^{1/2}\epsilon_e\Gamma$ (Sari et al. 1998), this condition yields:

$$\left(\frac{\nu_m}{1\ \mathrm{keV}}\right) \lesssim 3.3 \left(\frac{\epsilon_e}{0.5}\right)^{-1} \left(\frac{f(p)}{f(2.2)}\right)^{-1/2} \tag{19}$$

For our choice we have $\nu_m = 0.15$ keV at $t = 2.5$ s, while the right hand side of the above equation computed for $\epsilon_e = 8.8 \times 10^{-2}$ and $p = 2.05$ is equal to $\sim$ 66 keV. Thus, also the above condition is verified.

5. Conclusion

We have investigated on the possible origin of the high energy tail associated to GRB 081024B, exploring four main possibilities:

1. synchrotron or SSC component associated to the prompt burst emission (IS scenario);
2. SSC component associated to a delayed X-ray emission produced by late IS;
3. synchrotron component from the ES generating the afterglow emission;
4. SSC component from the ES generating the afterglow emission.

To derive the parameters of the models, we have considered the observational constraints coming from the prompt emission properties (scenario 1.), or from the late time X-ray observations (scenario 3.), or finally from the X-ray luminosity typically observed in short GRBs at 100 s after the burst (scenarios 2. and 4.), requiring to have an SSC component peaking around 1 GeV with a flux level comparable to the LAT sensitivity. We have shown that while scenarios 2. and 4. are viable explanations of the observed tail for a burst located at $z \sim 0.1$, the first one is ruled out due to substantial suppression of the high energy emission by pair production, while the third one is ruled out from the lack of a bright late-time X-ray afterglow. To have the high energy tail explained in a delayed IS scenario, the lately emitted shells should be characterized by a time variability of the order of 1 ms and a Lorentz factor of the order of $\Gamma = 140$. In the ES shock scenario, the high energy tail can be explained by assuming a flat spectrum, i.e. $p = 2.05$, and by requiring the short GRB to be powered by a fireball with an isotropic energy of the order of 10^{51} ergs, expanding in an ISM with density $n = 5$ cm^{-3}. We stress that scenarios 2. and 4., being related to the emission from a lately emitted shell (2.) or from the ES deceleration phase (4.), both offer a natural explanation for the observed temporal delay between the high energy tail and the main burst.

Acknowledgements. We thank Alessandra Galli for valuable discussions. A. Corsi is grateful to the Italian L'Oreal-UNESCO program "For Women in Science" for support. The authors acknowledge the support of ASI-INAF contract I/088/06/0.

References

Abdo, A. A. et al. 2009, Science, 323, 1688
Asano, K. & Inoue, S. 2007, ApJ, 671, 645
Baring, M. G. & Braby, M. L. 2004, ApJ, 613, 460
Chandra, P. et al. 2008, ApJ, 683, 924
Connaughton, V. et al. 2008, GCN, 8408
Corsi, C. & Piro, L. 2006, A&A, 458, 741
Corsi, C. et al. 2005, A&A, 438, 829
Dai, Z. G. & Lu, T. 2002, ApJ, 580, 1013
Fan, Y.-Z. 2009, to appear in MNRAS
Fan, Y.-Z. & Piran, T. 2008, Front. Phys. China, 3, 306
Fan, Y.-Z. et al. 2008, MNRAS, 384, 1483
Galli, A. & Piro, L. 2007, A&A, 475, 421
Galli, A. & Piro, L. 2008, A&A, 489, 1073
Galli, G. & Guetta, D. 2008, A&A, 480, 5
Ghisellini, G., Celotti, A., & Lazzati, D. 2000, MNRAS, 313, 1
Gou, l.-J. & Mészáros, P. 2007, ApJ, 668, 392
Guetta, D. & Granot, J. 2003, ApJ, 585, 865
Guidorzi, C. et al. 2008a, GCN, 8410
Guidorzi, C. et al. 2008b, GCN, 8416
Guidorzi, C. et al. 2008c, GCN, 8454
Guidorzi, C. et al. 2008d, GCN report, 178
Hanabata, Y. et al. 2008, GCN, 8444
Harrison, F. A. et al. 2001, ApJ, 559, 123
Li, Z. 2008, to appear in MNRAS, arXiv0810.2932L
Mészáros, P. & Rees, M. 1993, ApJ, 556, L37
Nakar, E. 2007, PhR, 442, 166
Ohno, M. et al. 2009, GCN, 9334
Omodei, N. 2008, GCN, 8407
Panaitescu, A. 2006, MNRAS, 367, L42
Panaitescu, A. & Mészáros, P. 2000, ApJ, 544, 17
Papathanassiou, H. & Mészáros, P. 1996, ApJ, 471, L91
Pe'er, A. & Waxman, E. 2004, ApJ, 613, 448
Pe'er, A. & Waxman, E. 2005, ApJ, 633, 1018
Pilla, R. P. & Loeb, A. 1998, ApJ, 494, L167
Sari, R. & Esin, A. A. 2001, ApJ, 548, 787
Sari, R. & Piran, T. 1999, ApJ, 520, 641
Sari, R., Piran, T., & Narayan, R. 1996, ApJ, 473, 204
Sari, R., Piran, T., & Narayan, R. 1998, ApJ, 497, L17
Scargle, J. D., Norris, J. P., & Bonnell, J. T. 1998, American Institute of Physics Conference Series, 181, 428
Wang, X.-Y., Li, Z., & Mészáros, P. 2006, ApJ, 641, 89
Wang, X.-Y. Z., Dai, Z. G., & Mészáros, P. 2009, to appear in ApJ Lett., arXiv0903.2086
Wei, D. M. & Lu, T. 1998, ApJ, 505, 252
Wei, D. M. & Lu, T. 2000, ApJ, 360, 13
You, Y. W., Liu, X. W., & Dai, Z. G. 2007, ApJ, 671, 637
Yu, Y. W. & Dai, Z. G. 2009, ApJ, 692, 133
Zhang, B. & Mészáros, P. 2001, ApJ, 559, 110
Zhang, B. et al. 2007, ApJ, 655, 989
Zou, Y.-C., Fan, Y.-Z., & Piran, T. 2008, to appear in MNRAS, arXiv:0811.2997v1

List of Objects

'GRB 081024B' on page 1
'GRB 081024B' on page 1
'GRB 081024B' on page 1
'GRB 081024B' on page 2
'GRB 081024B' on page 2
'GRB 081024B' on page 2
'GRB 081024B' on page 2
'GRB081024B' on page 2
'GRB 081024B' on page 2
'GRB 081024B' on page 3
'GRB 081024B' on page 3

‘GRB 081024B’ on page 4
‘GRB 081024B’ on page 4
‘GRB 081024B’ on page 4
‘GRB 081024B’ on page 5
‘GRB 081024B’ on page 6